JCTC Journal of Chemical Theory and Computation

Torsional Barriers and Equilibrium Angle of Biphenyl: Reconciling Theory with Experiment

Mikael P. Johansson*,†,‡ and Jeppe Olsen†

Lundbeck Foundation Center for Theoretical Chemistry, Aarhus University, DK-8000 Århus C, Denmark, and Department of Chemistry, University of Helsinki, Helsinki, Finland

Received May 22, 2008

Abstract: The barriers of internal rotation of the two phenyl groups in biphenyl are investigated using a combination of coupled cluster and density functional theory. The experimental barriers are for the first time accurately reproduced; our best estimates of the barriers are 8.0 and 8.3 kJ/mol around the planar and perpendicular conformations, respectively. The use of flexible basis sets of at least augmented quadruple-ζ quality is shown to be a crucial prerequisite. Further, to finally reconcile theory with experiment, extrapolations of both the basis set toward the basis set limit and electron correlation toward the full configuration-interaction limit are necessary. The minimum of the torsional angle is significantly increased by free energy corrections, which are needed to reach an agreement with experiment. The density functional B3LYP approach is found to perform well compared with the highest level *ab initio* results.

1. Introduction

From an electronic structure point of view, biphenyl ($C_{12}H_{10}$, see Figure 1) is a surprisingly challenging molecule. Especially pinpointing the energetics of the internal rotation around the central C−C bond connecting the two benzene units has proven problematic. The traditional picture of the interactions involved in deciding the torsional angle between the two twisted phenyl planes is that of an energetic competition between the favorable π-conjugation between the two planes and the steric repulsion between the adjacent hydrogens in *ortho*-position. Here we should mention that this interpretation of the counterbalancing interactions was recently challenged by Matta et al.,[1] who proposed that the hydrogen−hydrogen interaction would in fact be attractive and that the reason for nonplanarity instead is caused by an unfavorable lengthening of the central C−C bond when the planes become more coplanar. This view was later rejected in favor of the classical interpretation by Poater et al.[2] The debate is ongoing.[3] Anyhow, opposing interactions are involved, and therefore a theoretical approach that treats all important effects on equal footing is necessary for a reliable description of the potential energy surface.

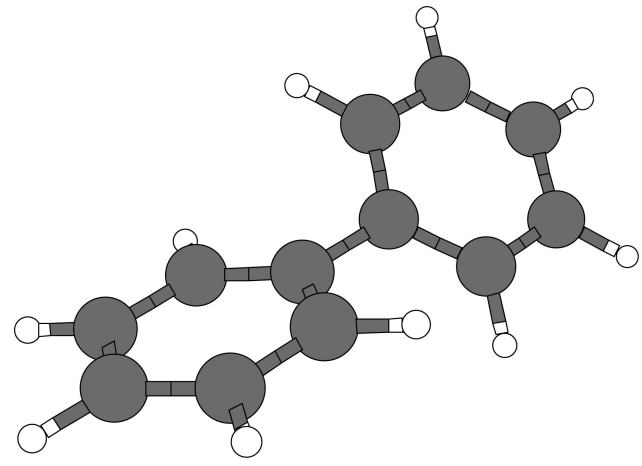

Figure 1. The equilibrium structure of biphenyl, $C_{12}H_{10}$. The figure was created with XMakemol.[4]

In the most recent gas-phase experiments, Bastiansen and Samdal estimated the barriers to be 6.0 ± 2.1 kJ/mol and 6.5 ± 2.0 kJ/mol around 0° and 90°, respectively,[5] while Almenningen et al. found the equilibrium angle to be 44.4 ± 1.2°.[6] The computational reproduction of the experimental barriers of torsion has hitherto proved to be difficult for

* Corresponding author e-mail: mikael.johansson@iki.fi.
† Aarhus University.
‡ University of Helsinki.

10.1021/ct800182e CCC: $40.75
Published on Web 08/08/2008

theoretical methods. *Ab initio* quantum chemical methods tend to give too high barriers, especially for the rotation around the planar conformation.[7−15] Recently, Sancho-García and Cornil[16] performed a thorough and systematic study of the energetics of the torsional potential of biphenyl. Using high-level correlated wave function methods, their best estimates of the barriers were still higher than those deduced from experiment. The 0° barrier was 2.4 kJ/mol beyond the experimental uncertainty. More importantly, the order of the barrier heights differed from experiment, with ΔE (0°) > ΔE (90°). The elusiveness of the experimental values has led to speculations about possible problems and ambiguities in the experimental interpretation.

While experimental problems naturally cannot be ruled out and were commented on already in the original work,[5] we set our goal to obtain a theoretical treatment that is as thorough as possible, by performing high-level electronic structure calculations, including all major effects. Hence, we explore the limits of all three dimensions of quantum chemical accuracy: *(i)* the amount of correlation energy accounted for, *(ii)* the completeness of the one-particle basis set (which Sancho-García and Cornil[16] identified as probably the largest source of error left in their study), and, last and least, *(iii)* the completeness of the Hamiltonian, that is, inclusion of relativity. As we will show, meticulous calculations allow us to finally reconcile theory with experiment, for the right reasons, without relying on compensating errors.

2. Methodology Overview

The geometries of biphenyl in various conformations have been obtained at the density functional theory (DFT) level,[17,18] within the generalized gradient approximation (GGA),[19] using the popular combination of Becke's three-parameter hybrid exchange functional[20] in connection with the Lee−Yang−Parr correlation[21] functional, B3LYP; the correlation of the uniform electron gas was modeled with the Vosko-Wilk-Nusair VWN5 formulation.[22] The doubly polarized triple-ζ quality basis-set, TZVPP,[23] was used during optimization. Final B3LYP and Hartree−Fock (HF)[24,25] energies were evaluated from extrapolated energies using Jensen's polarization consistent basis set series, pc-*n*.[26−29] Scanning of the potential energy surface (PES) of the relative torsional angle of the phenyl planes was done by optimizing all coordinates except the torsional angle. Additional geometry optimizations were performed using HF and second order Møller−Plesset perturbation theory (MP2),[30] within the density-fitting resolution of the identity formulation (RI-MP2).[31,32]

Correlated *ab initio* wave function (WF) energies were calculated using the B3LYP structures at the following levels of theory: MP2, the spin component scaled version of MP2 (SCS-MP2),[33] and coupled cluster (CC) including single and double excitations, CCSD,[34] as well as perturbative triples corrections, CCSD(T).[35] In general, the 1*s* orbitals of the carbon atoms were kept frozen, and Dunning's standard basis sets[36,37] of up to the augmented quadruple-ζ level, i.e., 1420 basis functions, were employed. Fully correlated calculations were performed with the weighted core-valence basis set of Peterson and Dunning.[38] Details on the use of basis sets are given in the discussion. The basis set limit was estimated by the two-point scheme of Halkier et al.[39] (eq 3). The full configuration-interaction limit was extrapolated from the CC values with Goodson's continued fraction method[40] (eq 4).

The zero point energies (ZPE) as well as the enthalpies ΔH and free energies ΔG at experimental temperature were estimated within the harmonic approximation, treating rotation and translation classically. The vibrational frequencies were calculated analytically[41] at the B3LYP/TZVPP level. Relativistic effects were computed at the B3LYP level with the one-step exact two-component relativistic Hamiltonian recently presented by Iliaš and Saue.[42]

Molecular symmetry was exploited to speed up the calculations. The planar (0°) conformation was assigned D_{2h} symmetry, and the perpendicular (90°) conformation D_{2d} (abelian C_{2v} where necessary). The intermediate torsion angle conformer calculations were performed in D_2 symmetry.

The correlated wave function calculations were performed with the Molpro 2006.1 package;[43−45] the Turbomole 5.91 program suite[46−51] was used for nonrelativistic DFT and all geometry optimizations; and relativistic calculations were performed with the Dirac package.[52] Default convergence and threshold parameters were employed, with the following, tighter exceptions: The Molpro aug-cc-pVQZ calculations used one- and two-electron integral thresholds of 10^{-15}; the Turbomole calculations used the "m4" type grid[53] and a self-consistent field (SCF) convergence criterion of 10^{-7} Hartree. Some basis sets were obtained via the convenient Basis Set Exchange portal.[54,55]

3. Results and Discussion

In this section, we begin by examining the pure, nonrelativistic electronic energies at 0 K of biphenyl. The relative energies of three conformations are studied: the equilibrium structure as well as the planar and perpendicular transition states. After that, various correction terms to the energies are discussed. These include relativistic effects, zero-point vibrational energies and thermal corrections, and the effect of correlating all electrons. Extrapolations to the basis set limits and electron correlation limits are performed. After this, we combine everything and report our best estimates of the final barriers of rotation. Finally, we discuss the equilibrium torsion angle.

3.1. Nonrelativistic Electronic Energies. We have calculated the torsional barriers over the planar, 0°, and the perpendicular, 90°, conformations, with various wave function methods. Several different basis sets have been used for single-point energy evaluations on the structures optimized at the B3LYP/TZVPP level. Full relaxation of the coordinates was allowed, with the exception of the torsional angle. In addition to the transition state structures, also the angle of the equilibrium structure was constrained, to the experimental value of 44.4°. A full optimization at the B3LYP level gives an angle of 39.5° at 0 K. The potential energy surface near the minimum is, however, very shallow, and the 44.4° conformation lies only 0.26 kJ/mol higher in energy. This is further discussed in Section 3.12, where thermal corrections are seen to have a large effect on the minimum angle.

Table 1. Computed Barriers of the Torsion around 0° and 90°, Using Selected Dunning Basis Sets[a]

	HF		MP2		SCS-MP2		CCSD		CCSD(T)	
	0°	90°	0°	90°	0°	90°	0°	90°	0°	90°
cc-pVDZ	12.82	5.40	12.23	7.68	12.24	6.73	11.34	6.56	10.89	7.23
aug-cc-pVDZ	12.05	4.57	9.86	7.45	10.15	6.45	9.77	6.08	9.23	6.67
cc-pVTZ	12.49	5.82	9.86	9.13	10.27	7.97	9.69	7.68	8.85	8.50
aug-cc-pVTZ	12.46	5.95	9.78	9.43	10.30	8.26	9.77	8.05	8.83	8.86
cc-pVQZ	12.56	5.88	9.65	9.33	10.14	8.13	9.64	7.90	8.68	8.74
aug-cc-pVQZ	12.53	5.81	9.35	9.31	9.89	8.12	9.41	7.92	8.39	8.76

[a] The barriers are given in kJ/mol.

Table 1 shows the barriers obtained with basis sets of increasing size. One can note that for all of the correlated wave function methods considered, the barrier at 90° seems to converge rather smoothly toward the aug-cc-pVQZ value, both when increasing the cardinal number of the basis set and when augmenting the basis with diffuse functions.

For the barrier around 0°, the situation is different. The barrier gets constantly lower compared to the perpendicular barrier, and, for CCSD(T), ΔE (0°) eventually falls below ΔE (90°), in agreement with the experimental results. However, there is still a notable lowering of the barrier when adding diffuse functions to the quadruple-ζ quality basis set, that is, when going from cc-pVQZ to aug-cc-pVQZ. At the CCSD(T) level, the difference is 0.3 kJ/mol. Therefore, the basis set limit cannot safely be considered to be reached.

We also want to stress, as has been done several times before, that correlated calculations at the cc-pVDZ level are highly unreliable, almost to the point of being useless. Little of the correlation energy inherent to a particular method is captured, and, what is worse, the amount is very different depending on conformation. As an example, the relative MP2 correlation energies at the cc-pVDZ level are −0.59 and +2.28 kJ/mol for the 0° and 90° barriers, respectively. This represents only 17% of the best estimate for the 0° conformation but 65% for the 90° conformation. Reasons for this, and the slower basis set convergence for the planar conformer in general, are discussed in more detail in connection with intramolecular basis set superposition error in Section 3.8.

3.2. Extrapolation toward the Basis Set Limit: Reference Energies. Using basis set extrapolation techniques, it is possible to obtain more accurate energies without performing prohibitively expensive calculations with larger basis sets. We begin by considering the reference Hartree−Fock energy.

A converged HF energy is naturally important, especially when very high accuracy is desired. With uncertainties in the reference energy, the incorporation of other, minute correction terms loses meaning. Although the correlation consistent series seems to be reasonably well converged also for the HF energy in Table 1, it is well-known that HF and DFT energies are not optimally represented by this series.[56,57] For this, we have employed Jensen's polarization-consistent basis sets, pc-*n*[26,27] and the augmented versions aug-pc-*n*.[28] The *n* in the basis set name indicates the polarization beyond the free atom. Thus, pc-1 for carbon is a double-ζ basis set with *s*, *p*, and *d* functions.

For the self-consistent field (SCF) energy extrapolations, both at the HF and B3LYP levels, we used two of the three-point schemes suggested by Jensen,[29] in connection with fully decontracted pc basis sets. Below, L_{max} is the highest angular momentum of the (carbon) basis set, N_s is the number of *s*-functions, and E_∞^{SCF}, B, and C are variables that need to be fitted using the energies of three consecutive pc-*n* basis sets:

$$E_\infty^{SCF} \approx E_{L_{max},N_s}^{SCF} - B(L_{max}+1)e^{-C\sqrt{N_s}} \quad (1)$$

The following, simpler formula, which does not take N_s as a parameter was also used:

$$E_\infty^{SCF} \approx E_{L_{max}}^{SCF} - B(L_{max})^{-C} \quad (2)$$

Table 2. Barriers Computed at the HF and B3LYP Levels Using Fully Decontracted Polarization Consistent Basis Sets, As Well As Selected Karlsruhe Basis Sets[a]

	HF		B3LYP	
	0°	90°	0°	90°
pc-1	13.57	4.22	9.16	7.07
aug-pc-1	15.16	5.35	9.38	7.88
pc-2	12.70	5.62	8.04	8.32
aug-pc-2	12.52	5.71	7.75	8.40
pc-3	12.50	5.79	7.76	8.48
aug-pc-3	12.49	5.80	7.76	8.49
pc-4	12.47	5.81	7.76	8.50
SVP	11.71	6.04	5.92	9.57
TZVPP	12.55	5.75	7.73	8.40
QZVPP	12.53	5.79	7.83	8.47

[a] Energies are in kJ/mol.

Table 2 shows the HF barriers computed with different pc basis sets; extrapolated values are found in Table 3. For comparison, we have also tested a few selected Karlsruhe basis sets[23,58,59] and in addition report B3LYP results.

The nice, smooth convergence of the barriers when climbing the pc-*n* ladder is noteworthy. The SCF energies, both for HF and B3LYP, are well converged at the pc-4 level. Both extrapolation formulas for pc-[2,3,4] give essentially the same barriers as the nonextrapolated value. The total energies are between 0.12 and 0.17 kJ/mol lower, though. The fitted C parameter for eq 1 is near 6 for all extrapolation combinations. This was noted in ref 29 and exploited for the construction of a two-point fitting scheme, the validity of which our results corroborate. For eq 2, the C parameter changes significantly when increasing L_{max}. For both equations, the B parameter assumes very varied values.

Also for the SCF energies, the double-ζ basis sets pc-1, aug-pc-1, and SVP[58] give quite poor barriers. The Dunning (aug)-cc-pVDZ basis sets actually perform significantly better, see Table 1. The sometimes unsatisfactory perfor-

Table 3. Extrapolated Values for the Barriers Computed at the HF and B3LYP Levels Using Fully Decontracted Polarization Consistent Basis Sets[a]

	HF				B3LYP			
	0°	90°	$\tilde{B}$	$\tilde{C}$	0°	90°	$\tilde{B}$	$\tilde{C}$
				Using Eq 1				
pc-[1,2,3]	12.48	5.80	1.45×10^5	5.42	7.73	8.49	1.61×10^5	5.45
aug-pc-[1,2,3]	12.50	5.74	9.19×10^5	5.74	7.77	8.49	1.07×10^6	5.79
pc-[2,3,4]	12.46	5.82	1.02×10^6	6.04	7.77	8.50	1.32×10^6	6.12
				Using Eq 2				
pc-[1,2,3]	12.43	5.83	1.52×10^0	5.85	7.66	8.52	1.60×10^0	5.90
aug-pc-[1,2,3]	12.52	5.83	1.45×10^0	5.86	7.79	8.52	1.54×10^0	5.92
pc-[2,3,4]	12.46	5.82	5.17×10^3	11.31	7.77	8.50	6.20×10^3	11.45

[a] The average values of the fitting parameters B and C are also reported for each extrapolation series. Energies are in kJ/mol.

mance of pc-1 has been noted earlier.[56] It is also interesting to note that contrary to the correlated WF energies, augmenting the double-ζ basis set degrades the relative energies between the 44.4° and 0° conformations quite significantly. Possible reasons for this are discussed in Section 3.8.

From the data in Table 3, one cannot clearly recommend one extrapolation scheme over the other. When extrapolating the pc-n, $n = 2,3,4$ series, the formulations give very similar energies. Some differences using the smaller basis sets can be noted, but neither method consistently outperforms the other. Using eq 2, the total pc-[2,3,4] energies are *ca.* 0.05 kJ/mol lower. For this specific series, eq 2 was found to perform slightly better also for the smaller systems in ref 29. Probably due to its simpler formulation, the numerical solutions were also more stable, whereas solving the system of equations arising from eq 1 on occasion required manual fine-tuning of the initial guesses to converge. Also, although unambiguous for biphenyl, deciding on the values of N_s in eq 1 is not always trivial.[29] For these reasons, we use the values obtained by eq 2 as our reference energies.

3.3. Extrapolation toward the Basis Set Limit: Correlation Energies. With a reliable reference energy established, we now turn our attention to the correlation energy. We have used the two-point extrapolation scheme of Halkier et al.,[39] which has proven to be robust and reliable. Below, X and Y are the (consecutive) cardinal numbers of the two basis sets used in the extrapolation, that is, 3 for a cc-pVTZ basis, etc.:

$$E_{\infty}^{\mathrm{corr}} \approx E_{XY}^{\mathrm{corr}} = \frac{E_X^{\mathrm{corr}} X^3 - E_Y^{\mathrm{corr}} Y^3}{X^3 - Y^3} \qquad (3)$$

In Table 4, extrapolation combinations are given for the various choices of basis sets. The nonextrapolated aug-cc-pVQZ barriers from Table 1 are reproduced for convenience. The extrapolation corroborates the findings in Section 3.1: The relative energies between the 44.4° and 90° conformations are converged. Extrapolation using the aug-cc-pVTZ and aug-cc-pVQZ bases, aug-cc-pV[T,Q]Z, gives almost the same barriers as those of the nonextrapolated aug-cc-pVQZ basis set. But as suspected, there is still a significant lowering of the barrier at 0°, with augmentation by diffuse function being critical. Part of the difference between the pure aug-cc-pVQZ and the extrapolated values comes from the nonconverged HF reference energy. The last row in Table 4 shows the barriers calculated using the extrapolated reference HF energy together with the correlation energy of the aug-cc-pVQZ basis. The difference compared to the extrapolated correlated energies decreases but is still significant. The magnitude of the lowering is indeed so large, ~0.4 kJ/mol, that one cannot rule out a further lowering by employing even larger basis sets.

Table 4. Barriers of the Torsion around 0° and 90°, Using Extrapolated Values from Two Basis Sets[a]

	MP2		SCS-MP2		CCSD		CCSD(T)	
	0°	90°	0°	90°	0°	90°	0°	90°
cc-pV[D,T]Z	8.98	9.56	9.55	8.30	9.11	7.97	8.10	8.84
aug-cc-pV[D,T]Z	9.57	9.56	10.18	8.32	9.60	8.17	8.48	9.08
cc-pV[T,Q]Z	9.35	9.37	9.90	8.14	9.47	7.95	8.41	8.81
aug-cc-pV[T,Q]Z	8.93	9.34	9.47	8.13	9.03	7.94	7.96	8.79
aug-cc-pVQZ	9.35	9.31	9.89	8.12	9.41	7.92	8.39	8.76
aug-cc-pVQZ(erE)	9.29	9.32	9.82	8.13	9.34	7.93	8.33	8.77

[a] For example, the extrapolated value from the cc-pVTZ and cc-pVQZ basis sets is denoted cc-pV[T,Q]Z. The extrapolated pc-[2,3,4] values have been used as reference HF energies. For comparison, the raw, nonextrapolated aug-cc-pVQZ values are reported; (erE) denotes that the extrapolated reference energy has been used. Energies are in kJ/mol.

Slightly surprisingly, the extrapolated cc-pV[D,T]Z relative energies are, for all methods, quite close to the aug-cc-pV[T,Q]Z energies. Fortuitously, the energy differences between cc-pVDZ and cc-pVTZ results apparently reproduce the right convergence behavior. All extrapolated results get the barrier order for CCSD(T) correct, with ΔE (0°) < ΔE (90°). This underlines the usefulness of extrapolation; significantly better relative energies can be obtained compared to the nonextrapolated raw energies.

3.4. Comparison of Correlated Methods. Comparing the different hierarchies of correlated wave function methods to the reference CCSD(T) data, a few points can be observed:

a. The MP2 method overestimates ΔE (0°), ΔE (90°) by 1.0 and 0.6 kJ/mol, respectively, but gives the correct ordering of the barriers.

b. The SCS-MP2 method overestimates ΔE (0°) by 1.5 kJ/mol and underestimates ΔE (90°) by 0.7 kJ/mol, which leads to an erroneous ordering of the barriers.

c. The CCSD method overestimates ΔE (0°) by 1.1 kJ/mol and underestimates ΔE (90°) by 0.8 kJ/mol, which again leads to an erroneous ordering of the barriers.

Triple excitations on top of the CCSD energies are important. Table 5 shows the basis set dependence of the triples contribution, (T). The 90° values again seem well converged, while a slight increase in the absolute magnitude

Table 5. Perturbative Triples Contributions with Different Basis Sets and Extrapolation Combinations[a]

	0°	90°
cc-pVDZ	−0.45	+0.67
aug-cc-pVDZ	−0.54	+0.59
cc-pVTZ	−0.85	+0.82
aug-cc-pVTZ	−0.94	+0.81
cc-pVQZ	−0.96	+0.84
aug-cc-pVQZ	−1.02	+0.84
cc-pV[D,T]Z	−1.00	+0.88
aug-cc-pV[D,T]Z	−1.11	+0.91
cc-pV[T,Q]Z	−1.05	+0.86
aug-cc-pV[T,Q]Z	−1.07	+0.85

[a] Energies are in kJ/mol.

of the correction for the barrier at 0° is still present, when comparing the aug-cc-pVQZ and the aug-cc-pV[T,Q]Z results. The difference is however only 0.05 kJ/mol, much lower than the corresponding difference for the total barrier. This is in line with previous findings where the basis set dependence of the perturbative triples has been shown to be less severe than for CCSD single and double excitations.[60,61]

The triples correction contributes with different sign to the two barriers; the 0° barrier is lowered by ∼1.1 kJ/mol, while the 90° barrier is raised by ∼0.9 kJ/mol. This implies that triple excitations are the more abundant, the more planar the conformation is. A possible explanation for this is that as the planarity of the molecule increases, the electron density of *ortho*-hydrogens overlaps increasingly, giving more opportunities for triple excitations to occur.

The relatively good performance of MP2 is apparently rooted in the quite large triple excitation corrections when going from CCSD to CCSD(T). This is naturally something that cannot be represented at the second-order perturbation level, where only double excitations contribute to the energy. Thus the good agreement comes from a cancelation of errors. This also explains the failure of SCS-MP2, where the only difference to standard MP2 is that the same-spin and opposite-spin contributions to the correlation energy are scaled differently. In essence, no information about the triples contribution enters. SCS-MP2 was devised partly to damp the usual overestimation of long-range same-spin correlation in MP2.[33] In the case of biphenyl, this overestimation of MP2 fortuitously mimics the triples contribution. Thus, without artificially overestimated dispersion, the SCS-MP2 energies become worse and closer to the CCSD results.

The magnitude of the triples correction entices caution toward the adequacy of treating the triples in a perturbative manner, a full triples consideration might provide additional contributions to the relative energies. In addition to not going beyond perturbative triple excitations, CCSD(T) does not account for a possible multireference character present in the molecule (except indirectly, via the reasonably high percentage of correlation energy recovered). This is expected to be a minor omission, however. Diagnostics devised to quantify the reliability of a single-reference treatment support this view. The $T1$ diagnostic by Lee and Taylor[62] of the CCSD solution was in all cases found to be below 0.011. The $D1$ diagnostic by Janssen and Nielsen[63] was always below 0.030. Thus it appears quite safe to omit an explicit treatment of multiple reference configurations. However, as will be shown in Section 3.6, extrapolation toward the full configuration-interaction limit still has an appreciable effect on the barrier heights.

3.5. Core−Core and Core−Valence Correlation. To explore the error introduced by keeping the 1*s* orbital of carbon uncorrelated in the WF calculations, we performed calculations with all electrons correlated. This was done using the weighted core-valence basis sets of Peterson and Dunning.[38] Computational resources limited this study to the double- and triple-ζ basis sets, cc-pwCVDZ and cc-pwCVTZ, and subsequent extrapolation, although some cc-pwCVQZ calculations were performed, as discussed at the end of this section. The effect of correlating the core electrons in a given basis set was obtained by comparing energies with and without correlating the 1*s* electrons of the carbons. Table 6 shows that the relative corrections that core-correlation introduce are small but nonvanishing. The extrapolation was performed with eq 3 using only the core-correlation contribution, *not* the full correlation energy. The extrapolated cc-pwCV[D,T]Z values are arguably, with the assumption that the core correlation energy follows the same convergence pattern as the total correlation energy, the most accurate. For all methods, core correlation is thus seen to raise both barriers slightly, the effect on the 0° conformation being more pronounced.

The double-ζ cc-pwCVDZ basis set is again much too small to give reasonable results for any of the correlated WF methods. Even if the correction is small, its magnitude and even its sign change when using larger basis sets. Thus, for estimating core-correlation effects the use of at least a triple-ζ basis is mandatory, lest the "correction" turns to degradation.

The basis set problems are again more severe for the planar conformation, while the convergence of the 90° barrier is much smoother. Thus the uncertainties in the core-correlation corrections for the 0° barrier are bigger than for the perpendicular; the 0° corrections should probably be even slightly more positive, i.e., raise the barrier slightly more. To test this, we performed calculations with the quadruple-ζ cc-pwCVQZ basis set. This basis set was too large for fully correlated computations on the 44.4° conformer with available resources, so only the relative corrections between the planar and perpendicular conformers could be obtained. Comparing the barriers obtained at the cc-pwCV[D,T]Z and cc-pwCV[T,Q]Z levels, it was found that the 0° barrier is indeed slightly raised when using the more complete extrapolation: For MP2 and SCS-MP2 by 0.02 kJ/mol and for CCSD and CCSD(T) by 0.03 kJ/mol, compared to the 90° conformer. As the core-correlation contribution to the 90° barrier seems quite converged already at the cc-pwCV[D,T]Z level, much of this would likely be transferable also to the relative energies between the 0° and 44.4° conformations.

Also for core-correlation, the two-point extrapolation scheme, eq 3, at least in this case, captures more of the correlation energy than the raw-values of a basis set one step ahead in the series. The relative energies are of comparable accuracy, that is, cc-pwCV[D,T]Z gives essentially the same relative energies as cc-pwCVQZ. The relative core-correlation at the CCSD(T) level is also almost the same as for

Table 6. Relative Core-Correlation Corrections to the Torsion around 0° and 90°, Using the Weighted Core-Correlation Basis Sets[a]

	MP2		SCS-MP2		CCSD		CCSD(T)	
	0°	90°	0°	90°	0°	90°	0°	90°
cc-pwCVDZ	−0.00	0.02	−0.06	0.01	−0.03	0.03	−0.04	0.02
cc-pwCVTZ	0.09	0.03	0.08	0.02	0.05	0.04	0.04	0.03
cc-pwCV[D,T]Z	0.13	0.04	0.11	0.02	0.09	0.05	0.08	0.03

[a] cc-pwCV[D,T]Z again denotes extrapolated values. Energies are in kJ/mol.

Table 7. Barriers of the Torsion around 0° and 90°, Calculated with the Continued-Fraction CC Method (CC-cf), Using the Best Estimates of the Total Energies at the HF, CCSD, and CCSD(T) Levels[a]

	0°	90°
CC-cf	7.88	8.94
CCSD(T)	8.04	8.83

[a] Also shown are CCSD(T) barriers including core-correlation. Energies are in kJ/mol.

CCSD, indicating that triple excitations from the core are not significant for the relative energies. A more complete dissertation of the cc-pwCVQZ results can be found in the Supporting Information.

3.6. Extrapolation toward the Full Configuration-Interaction Limit. With the best estimates for the electronic energies at different levels of theory available, we next proceed to extrapolation of the coupled cluster series toward completeness. For this, we have employed the continued fraction method of Goodson (CC-cf),[40] devised to provide near full configuration-interaction (FCI) energies. Below, $\delta_1 = E$ [HF], $\delta_2 = E$[CCSD] − E[HF], and $\delta_3 = E$[CCSD(T)] − E[CCSD]:

$$E[\text{CC-cf}] = \frac{\delta_1}{1 - \dfrac{\delta_2/\delta_1}{1 - \delta_3/\delta_2}} \tag{4}$$

For HF, the pc-[2,3,4] energies were used; for CCSD and CCSD(T), the aug-cc-pV[T,Q]Z energies with cc-pwCV[D,T]Z core-correlation contributions added were used. We note that all conformations were treated individually, after which the relative energies were computed.

Table 7 shows the barriers as obtained with eq 4 and represents our best estimates for the nonrelativistic electronic energies at 0 K. Compared to the CCSD(T) results, the barrier at 0° is lowered slightly more, while the 90° barrier is raised.

3.7. The Effect of Relativity. To check, and possibly rule out the effect of relativity on the barrier heights, we have performed relativistic all-electron calculations at the B3LYP level, using the fully decontracted TZVPP basis set, treated as Cartesian. Table 8 shows the barriers at the nonrelativistic Lévy-Leblond level[64] and using a one-step exact two-component relativistic Hamiltonian (X2C).[42]

The barriers are seen to be virtually unaffected by relativity. Even with the speed of light artificially halved to 0.5c, only a minute enhancement of the relativistic corrections is observed. An even more rigorous treatment of relativity, beyond X2C, might still have a small effect on the relative energies, but, for practical purposes, relativity can safely be considered not to contribute to the barrier heights in biphenyl.

Table 8. Barriers of the Torsion around 0° and 90°, Calculated at the B3LYP Density Functional Level, Using the Decontracted TZVPP Basis Set, at Nonrelativistic Lévy-Leblond (NR) and One-Step Exact Two-Component Relativistic (X2c) Levels[a]

	0°	90°
NR	7.98	8.39
X2C	7.99	8.39
X2C(0.5c)	7.83	8.38

[a] (0.5c) denotes calculations done with the speed of light halved. Energies are in kJ/mol.

3.8. Intramolecular Basis Set Superposition Error. As discussed above, the convergence toward the basis set limit is much slower for the planar conformation compared to that of the perpendicular. This has previously been attributed to the more demanding basis set requirement for describing the dispersion interaction in planar biphenyl.[11] In this Section, our working hypothesis will be that much of the difference instead arises from intramolecular basis set superposition error (BSSE).

Intramolecular BSSE is more difficult to assess than intermolecular BSSE between two fragments,[65−67] where the counterpoise (cp) correction scheme[68] has become a *de facto* standard. Jensen used an approach analogous to cp in a study of the BSSE for relative energies between different conformers of the same molecule.[66] When comparing the relative energies between the conformers, the logical suggestion was to explore the BSSE by the combined basis set of both conformers, that is, by inserting dummy, ghost atomic centers at the positions the other conformer would occupy, where the conformations superimposed. In the spirit of Jensen's method, we will compare these values with the results obtained in the normal basis sets, consisting of functions only on the atoms.

For simplicity, we have only considered the relative energies between the planar and perpendicular conformations. With this combination, the basis sets are augmented by 8 ghost centers, corresponding to the four carbons and four hydrogens that would stick out of the plane of one of the phenyl rings, if the structures would be superimposed. Figure 2 shows the situation for the planar conformer. Although the optimized geometries were used in the calculations, we have assumed that the rest of the atoms are located at the same relative positions in the two conformers, so as not to add dummy centers that nearly coincide with the atoms. The calculations were performed in C_{2v} symmetry.

Table 9 shows the relative energies, with and without corrections for BSSE. For the double-ζ basis sets, the addition of the ghost centers leads to a significant lowering of the 0° energy compared to the 90°. When going to the

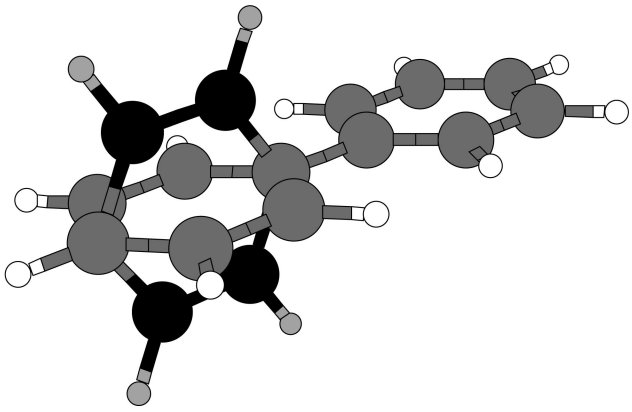

Figure 2. The planar conformation of biphenyl, with the ghost atom centers defined by the perpendicular conformation shown in black and gray.

Table 9. Relative Energies between the 0° and 90° Conformations, Calculated with Selected Basis Sets[a]

	HF	MP2	SCS-MP2	CCSD	CCSD(T)
cc-pVDZ	7.42	4.55	5.51	4.78	3.66
cc-pVDZ(cp)	6.61	1.67	3.20	3.00	1.42
Δ(cp)	−0.81	−2.88	−2.31	−1.78	−2.24
aug-cc-pVDZ	7.48	2.40	3.70	3.63	3.32
aug-cc-pVDZ(cp)	6.05	−0.27	1.38	1.21	−0.45
Δ(cp)	−1.43	−2.67	−2.32	−2.42	−3.77
cc-pVTZ	6.66	0.73	2.30	2.00	0.35
cc-pVTZ(cp)	6.62	0.58	2.25	1.92	0.15
Δ(cp)	−0.04	−0.15	−0.05	−0.08	−0.20
cc-pV[D,T]Z	-	−0.58	1.25	1.14	−0.74
cc-pV[D,T]Z(cp)	-	0.13	1.87	1.49	−0.37
Δ(cp)	-	+0.71	+0.62	+0.35	+0.37
aug-cc-pVQZ	6.72	0.04	1.77	1.49	−0.37
aug-cc-pV[T,Q]Z	-	−0.41	1.34	1.09	−0.83

[a] (cp) denotes that the basis set has been augmented by functions at the ghost centers of the other conformation. Δ(cp) is the difference between the normal and the (cp) basis sets. Energies are in kJ/mol; a positive value denotes that the 0° energy is higher.

cc-pVTZ basis set, things look better, and the difference between corrected and uncorrected energies becomes reasonably small.

An anomaly can be found in the extrapolated cc-pV[D,T]Z values, where the cp corrected energy differences are much further from the best estimates compared to the noncorrected ones, even though the cp-corrected basis sets are more complete. This also shows up as an artificially large BSSE correction, Δ(cp), which even has the "wrong" sign. The underlying reason is the fortuitously good performance of the cc-pV[D,T]Z energies, as discussed in Section 3.3; the extrapolated cc-pV[D,T]Z(cp) values are better than the raw cc-pVTZ(cp) values, as they are expected to be.

It is difficult to divide the energy differences between the normal and cp-augmented basis sets into components arising from just a larger flexibility of the basis set and BSSE. The fact that the difference decreases significantly when going from double-ζ to larger basis sets does suggest that a major part in fact is due to BSSE. A possible explanation for the origin of BSSE, which favors the 90° conformation over the 0° conformation, could be the following. In the planar conformation, basis functions are present only in the plane of the molecule. For the perpendicular conformation, the centers are naturally present in all three dimensions. Thus, in the perpendicular case, the phenyl planes can to an extent utilize basis functions from the other plane to describe the space above (and below) their own plane. This suggestion is supported by the fact that, for all methods save MP2, the correction term is bigger for aug-cc-pVDZ than cc-pVDZ: With augmented diffuse functions on the centers, they extend more efficiently over to the top (and bottom) of the other plane. This would explain the much slower convergence of the energy in the planar conformer, where the space above the planes has to be described only by basis functions in the plane. For the same reason, the performance of the normal augmented double-ζ basis sets compared to the nonaugmented is poorer, as seen also for the pc-1 basis set in Section 3.2.

Much of the poor performance of the smaller basis sets in describing the relative energy of the planar and twisted conformers thus comes not from an intrinsically poorer description of the planar system but from a better possibility of the twisted conformers to "borrow" basis functions from the opposite plane. From Table 9, one can also note the usual observation that the BSSE is more pronounced for the correlated WF methods compared to HF.

3.9. Zero-Point Vibrational Energy and Thermal Corrections. In this section we consider the zero-point vibrational energy (ZPE) contributions to the barriers. The experimental values were measured at approximately the nozzle temperature of 401 K,[6] while the reported values for the potential barriers refer to absolute zero.[5] Nevertheless, it is of interest to explore the temperature dependence of the energetics, so we have also explored finite temperature effects on the barriers.

We consider the vibrational contributions to the thermal energy corrections with two different approaches. The basis for this is the observation that internal coordinate analysis shows the lowest vibrational frequency consistently to correspond almost purely to the internal rotation of the phenyl planes. This frequency becomes imaginary sufficiently far from equilibrium and naturally is imaginary also at the transition states at 0° and 90° angles. When calculating the ZPE, imaginary frequencies do not contribute to the sum over vibrations, lowering the ZPE. In general, the imaginary vibrations of transition states do not directly match a vibration in the ground-state geometry, but, in the special case here, there is a one-to-one correspondence. Therefore, it might be motivated to remove the lowest vibration also from the ZPE and vibrational contribution to the enthalpy (H) and free energy (G). A similar approach was discussed previously by Dos Santos et al.[69] We leave this option to the reader, but, subsequently in this work, we will consider the traditional method of including all real vibrations. Another approach would be to treat the internal rotation of the phenyl planes as a hindered rotation, as the barrier heights of *ca.* 8 kJ/mol are comparable to k_BT, 3.3 kJ/mol at experimental temperature.

In Table 10, the ZPE as well as relative enthalpies and free energies at the experimental temperature are shown, using both approaches discussed above, obtained at the B3LYP/TZVPP level. The ZPE has a notable effect on

Table 10. Lowest Frequencies (ν_1), Zero-Point Energies (ZPE), Relative Enthalpies (ΔH), and Free Energies (ΔG) for Biphenyl with Different Torsional Angles[a]

	all real freqs			3N−7 highest freqs		
	0°	44.4°	90°	0°	44.4°	90°
ν_1	80.5 *i*	61.0	55.3 *i*			
ZPE	475.80	475.68	475.02	475.80	475.32	475.02
ΔZPE	+0.12	0	−0.66	+0.49	0	−0.30
ΔH (401 K)	518.14	521.04	517.58	518.14	517.69	517.58
$\Delta\Delta H$	−2.90	0	−3.46	+0.45	0	−0.12
ΔG (401 K)	352.28	345.92	349.98	352.28	350.98	349.98
$\Delta\Delta G$	+6.36	0	+4.06	+1.30	0	−1.00

[a] Values calculated using all real frequencies are shown together with values calculated using all except the lowest frequency. Calculated at the B3LYP/TZVPP level. Frequencies are in cm^{-1}; energies are in kJ/mol.

the relative energies. As expected, the barriers are raised if the lowest vibration is consistently omitted. This is especially pronounced in the case of enthalpy and free energy corrections. Without the frequency of the internal rotation, there is a very small change between the relative zero point energies and the enthalpies, indirectly confirming that other vibrational modes are largely independent of the rotation.

It should be noted that we have chosen not to scale the vibrational frequencies, a common procedure used to approximate the effects of anharmonicity. In this case, it is not clear that scaling would provide an overall improvement of the frequencies, so adding an extra empirical scaling factor is not really motivated. Some inherent uncertainty in the computed zero-point energies and the thermal corrections based on the vibrations thus exists. Compared to the other remaining sources of uncertainty, this is probably the most significant.

3.10. The Effect of Geometry on the Relative Energies. All energetics discussed in previous sections are based on single-point evaluations on geometries optimized at the density functional B3LYP level. Although expected to be highly realistic, it is difficult to estimate exactly how good the geometries are, without performing full optimizations at a sufficiently high *ab initio* level. This is however, for the time being, beyond reasonable computational resources. For this reason, it is of interest to examine how sensitive the relative energies are with respect to the exact geometries of the 0°, 44.4°, and 90° conformations.

To explore this, we have reoptimized the geometries at Hartree−Fock and the RI-MP2 level, with subsequent single point energy calculations. The geometry optimizations used the same basis set as for the B3LYP geometries, i.e., TZVPP. Table 11 shows the relative cc-pVTZ energies at different levels of theory, based on geometries optimized at the B3LYP, MP2, and HF levels.

Some differences in the barriers can be noted, although none are very large. Even the barriers based on HF geometries deviate less than 0.2 kJ/mol in the case of correlated WF methods. The differences are largest for the HF and MP2 energies, where for the specific method more optimal geometries apparently play an especially prominent role. Reassuringly, the coupled cluster barriers are very similar for the electron correlation including B3LYP and MP2 geometries. We note that the total CCSD(T)/cc-pVTZ energies are *ca.* 0.5 kJ/mol lower when using the MP2 geometries instead of the B3LYP geometries, suggesting the MP2 geometries to be slightly superior. Again, the planar conformation exhibits the largest sensitivity, also with respect to geometries. However, all-in-all, even more accurate geometries are expected to have a very minor effect on the relative barriers.

3.11. Best Estimates of the Torsional Barriers. With values for all contributions to the barriers at zero temperature available, we are now able to sum them up. Table 12 summarizes the work. The best estimate values of the barriers are $\Delta E(0°) = 8.0$ kJ/mol, and $\Delta E(90°) = 8.3$ kJ/mol. Thus, we have succeeded in bringing the barriers to within the reported experimental uncertainty, reconciling theory with experiment. Although some uncertainties remain in the calculated values, the most important being *(i)* the zero-point energy and *(ii)* the remaining basis-set effect for $\Delta E(0°)$, we are fairly confident that the experimental values of 6.0 ± 2.1 and 6.5 ± 2.0 kJ/mol for the potential energy at 0° and 90°, respectively, are at the low end.

3.12. The Experimental vs Computed Torsional Angle. Finally, we turn to the equilibrium torsional angle. To pinpoint the exact minimum, the potential energy was calculated at 1° intervals between 33° and 51°. The correlated WF energies were obtained with the aug-cc-pVDZ and aug-cc-pVTZ basis sets, with subsequent extrapolation (aug-cc-pV[D,T]Z) as discussed in previous sections. The Hartree−Fock reference energies and B3LYP energies were obtained with the doubly polarized quadruple-ζ QZVPP[59] basis set. On top of the 0 K energies, thermal corrections were added, based on frequency calculations at the B3LYP/TZVPP level. The obtained energies were then fitted to a harmonic function of the usual form $E(\phi) = a \times (\phi\text{-}\phi_0)^2 + c$, with a, ϕ_0, and c free parameters, and ϕ_0 the resulting minimum torsion angle. To ensure that the region of the fit was as harmonic as possible, the final fit was performed using only points within 6° of the minimum angle, that is, using the 12 closest data points. Limiting the number of data points changed the angle very little, on average less than 0.1°, but resulted in slightly better fits.

Table 13 shows the calculated equilibrium angles at different levels of theory. The energy difference between the minimum angle and the 44.4° conformations, based on the fitted harmonic functions, are also shown. In Figure 3, the resulting curves for the electronic energy at the CC-cf, CCSD(T), and B3LYP levels are drawn. All correlated methods are in close agreement, giving a minimum angle of 38.8−41.0°, while the Hartree−Fock angle is much larger. The values and the curves are slightly shifted relative to each other, consistent with the relative energies of the 0° and 90° barriers at each level of theory. As for the energies, one can note that MP2 agrees quite well with the CC-cf and CCSD(T) results, both concerning the angle and the difference to the 44.4° conformation; SCS-MP2 again degrades both numbers. Also B3LYP fares well in the competition.

The experimentally measured[6] torsion angle of 44.4 ± 1.2° is significantly larger than the theoretical values at zero temperature; finite temperature effects can be expected to

Table 11. Torsional Barriers Based on Geometries Obtained at the B3LYP, MP2, and HF Levels of Theory, Using the cc-pVTZ Basis Set[a]

	HF		MP2		SCS-MP2		CCSD		CCSD(T)	
optimization level	0°	90°	0°	90°	0°	90°	0°	90°	0°	90°
B3LYP	12.49	5.82	9.86	9.13	10.27	7.97	9.69	7.68	8.85	8.50
MP2	12.27	5.78	9.99	9.11	10.32	7.94	9.65	7.69	8.86	8.52
HF	12.23	5.95	10.00	9.00	10.37	7.90	9.78	7.69	9.04	8.45

[a] Energies are in kJ/mol.

Table 12. Torsional Barriers at 0 K, Including All Corrections Considered: Nonrelativistic Electronic Energy (E(0 K), Including Core-Correlation), Relativistic Correction (RC), and Zero-Point Energy (ZPE)[a]

	CC-cf		CCSD(T)		B3LYP	
	0°	90°	0°	90°	0°	90°
E(0 K)	7.878	8.942	8.037	8.825	7.765	8.498
RC	+0.013	−0.002	+0.013	−0.002	+0.013	−0.002
ZPE	+0.120	−0.664	+0.120	−0.664	+0.120	−0.664
total	8.01	8.28	8.17	8.16	7.90	7.83

[a] The best-estimate continued-fraction barriers (CC-cf) are compared to those of CCSD(T) and B3LYP. Energies are in kJ/mol.

Table 13. Equilibrium Angle of Biphenyl Calculated at Different Levels: Electronic Energy at 0 K, and with Corrections for Zero-Point Energy (ZPE), Enthalpy (ΔH), and Free Energy (ΔG) at 401 K (CC-cf/B3LYP Level Only)[a]

	$\angle_{min}$	ΔE(44.4°)
Electronic Energy at 0 K		
HF	45.5°	0.01
MP2	39.6°	0.27
SCS-MP2	41.0°	0.13
CCSD	40.6°	0.15
CCSD(T)	39.0°	0.32
CC-cf	38.8°	0.36
B3LYP	39.4°	0.26
CC-cf with Correction Terms		
ZPE	40.0°	0.20
ΔH	39.6°	0.27
ΔG	45.8°	0.01

[a] The energy differences to the 44.4° angle conformation are also given, in kJ/mol.

be important. Figure 4 shows the potential energy curve calculated at the CC-cf level, with thermal corrections at the B3LYP level added. From Table 13 one sees that zero-point energy and enthalpy corrections increase the angle but only by *ca*. 1°. Accounting for entropy effects via the free energy ΔG, on the other hand, increases the angle significantly, by 7.0° to 45.8°.

Even with free energy accounted for, the computed equilibrium angle lies outside the experimental error bars, being slightly larger than the measured angle. The approximations used in the computations should be kept in mind. As discussed in relation with the relative energies between the 0° and 90° conformations, using larger basis sets would shift the curves slightly toward a lower angle, most likely nudging the equilibrium angle to within experimental error. Although this would bring the calculated angle in agreement with experiment, a probably larger source of error is the free energy correction itself. This has been

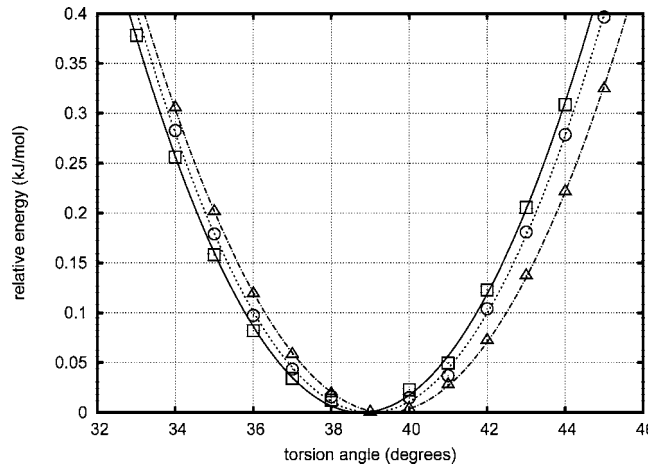

Figure 3. Potential energy curves near equilibrium, based on electronic energies at 0 K, calculated at the CC-cf (boxes), CCSD(T) (circles), and B3LYP (triangles) levels. The curves represent the harmonic potential fitted to the individual data points.

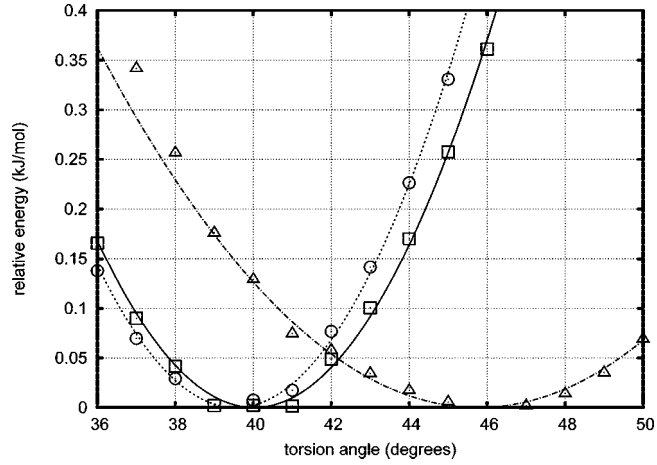

Figure 4. Potential energy curves near equilibrium, calculated at the CC-cf/B3LYP level. The electronic energies have been corrected for zero-point energy (boxes), enthalpy (circles), and free energy (triangles) at 401 K. The curves represent the harmonic potential fitted to the individual data points.

approximated via the vibrational frequencies that themselves contain uncertainties as discussed in Section 3.9. The effect of these approximations on the angle is difficult to predict, and a shift in either direction is possible. Further, all the energy curves are very shallow around the minimum, especially so the free energy surface. Small changes in the energies would have a notable effect on the angle. We are however fairly confident that the zero temperature angle is much smaller than the experimentally measured one. To

reproduce the measured angle, entropy and free energy are thus seen to be compulsory ingredients of the computational recipe.

4. Conclusions and Outlook

We have reported accurate calculations of the barriers of rotation around the central bond in biphenyl. In contrast to previous studies, we have shown that the experimentally inferred barriers *can* be reproduced, if sufficiently sophisticated methodology is employed. Our calculated best estimates for the barriers are $\Delta E(0°) = 8.0$ and $\Delta E(90°) = 8.3$ kJ/mol, while the values estimated from experimental data[5] were $\Delta E(0°) = 6.0 \pm 2.1$ and $\Delta E(90°) = 6.5 \pm 2.0$ kJ/mol. Although the calculated barriers fit within the reported experimental uncertainty, with the same order, the expected accuracy of our results strongly suggests that the true values are close to the upper limit of the error bars reported.

The basis set dependence of the barriers, especially around 0°, is high. Even augmented quadruple-ζ basis sets are insufficient; the use of extrapolation techniques are compulsory. This is the case also for the electron correlation treatment, where an extrapolation toward the full configuration-interaction limit is necessary, as the coupled cluster CCSD(T) approach still has a bias toward twisted conformations.

The equilibrium angle of biphenyl was investigated, and free energy corrections were found to be necessary to widen the computed angle toward the experimentally measured value[6] of $44.4 \pm 1.2°$. Due to the shallowness of the potential near minimum, the calculated value of 45.8° is, however, very sensitive to small errors and uncertainties in the computed energies.

Our results can readily serve as a basis for future benchmark calculations for various theoretical treatments. The reported standard, canonical CCSD(T) results, obtained with basis sets up to the augmented quadruple-ζ level (aug-cc-pVQZ), are among the largest performed to date. The nature of biphenyl, having a highly delocalized electronic structure, should prove an interesting test case for, e.g., local *ab initio* correlation methods and other approximate methods aiming toward a lower computational scaling. To this end, we provide the structures and total energies as Supporting Information.

For the computationally less demanding density functional approach, the intricate competition between different chemical interactions makes for a delicious challenge, especially for nonempirical functionals that have to rely on a good description of the chemistry and physics involved, without the help of fitted parameters. Indirectly, the B3LYP functional was already benchmarked here and found to agree well with the highest-level extrapolated *ab initio* results and experiment. Its good performance could be considered somewhat fortuitous, however, due to the empirical nature of the functional.

Acknowledgment. We are grateful to Prof. Svein Samdal, Dr. Frank Jensen, and Dr. Michael Patzschke for discussions. CSC—The Finnish IT Center for Science—provided abundant computational resources.

Supporting Information Available: Details, atomic coordinates, and total energies. This material is available free of charge via the Internet at http://pubs.acs.org.

References

(1) Matta, C. F.; Hernandéz-Trujillo, J.; Tang, T.-H.; Bader, R. F. W. Hydrogen-Hydrogen Bonding: A Stabilizing Interaction in Molecules and Crystals. *Chem. Eur. J.* **2003**, *9*, 1940–1951.

(2) Poater, J.; Solà, M.; Bickelhaupt, F. M. Hydrogen-Hydrogen Bonding in Planar Biphenyl, Predicted by Atoms-In-Molecules Theory, Does Not Exist. *Chem. Eur. J.* **2006**, *12*, 2889–2895.

(3) Pacios, L. F. A theoretical study of the intramolecular interaction between proximal atoms in planar conformations of biphenyl and related systems. *Struct. Chem.* **2007**, *18*, 785–795.

(4) Hodges, M. P. XMakemol: a program for visualizing atomic and molecular systems, version 5, 2001. See http://www.non-gnu.org/xmakemol/(accessed June 19, 2008).

(5) Bastiansen, O.; Samdal, S. Structure and barrier of internal rotation of biphenyl derivatives in the gaseous state. Part 4. Barrier of internal rotation in biphenyl, perdeuterated biphenyl and seven non-ortho-substituted halogen derivatives. *J. Mol. Struct.* **1985**, *128*, 115–125.

(6) Almenningen, A.; Bastiansen, O.; Fernholt, L.; Cyvin, B. N.; Cyvin, S. J.; Samdal, S. Structure and barrier of internal rotation of biphenyl derivatives in the gaseous state Part 1. The molecular structure and normal coordinate analysis of normal biphenyl and perdeuterated biphenyl. *J. Mol. Struct.* **1985**, *128*, 59–76.

(7) Häfelinger, G.; Regelmann, C. Refined ab initio 6−31G split-valence basis set optimization of the molecular structures of biphenyl in twisted, planar, and perpendicular conformations. *J. Comput. Chem.* **1987**, *8*, 1057–1065.

(8) Tsuzuki, S.; Tanabe, K. Ab Initio Molecular Orbital Calculations of the Internal Rotational Potential of Biphenyl Using Polarized Basis Sets with Electron Correlation Correction. *J. Phys. Chem.* **1991**, *95*, 139–144.

(9) Rubio, M.; Merchán, M.; Ortí, E. The internal rotational barrier of biphenyl studied with multiconfigurational second-order perturbation theory (CASPT2). *Theor. Chim. Acta* **1995**, *91*, 17–29.

(10) Karpfen, A.; Choi, C. H.; Kertesz, M. Single-Bond Torsional Potentials in Conjugated Systems: A Comparison of ab Initio and Density Functional Results. *J. Phys. Chem. A* **1997**, *101*, 7426–7433.

(11) Tsuzuki, S.; Uchimaru, T.; Matsumura, K.; Mikami, M.; Tanabe, K. Torsional potential of biphenyl: Ab initio calculations with the Dunning correlation consisted basis sets. *J. Chem. Phys.* **1999**, *110*, 2858–2861.

(12) Arulmozhiraja, S.; Fujii, T. Torsional barrier, ionization potential, and electron affinity of biphenyl–A theoretical study. *J. Chem. Phys.* **2001**, *115*, 10589–10594.

(13) Grein, F. Twist Angles and Rotational Energy Barriers of Biphenyl and Substituted Biphenyls. *J. Phys. Chem. A* **2002**, *106*, 3823–3827.

(14) Grein, F. New theoretical studies on the dihedral angle and energy barriers of biphenyl. *J. Mol. Struct. (Theochem)* **2003**, *624*, 23–38.

(15) Grein, F. Influence of diffuse and polarization functions on the second-order Møller-Plesset optimized dihedral angle of biphenyl. *Theor. Chem. Acc.* **2003**, *109*, 274–277.

(16) Sancho-García, J. C.; Cornil, J. Anchoring the Torsional Potential of Biphenyl at the ab Initio Level: The Role of Basis Set versus Correlation Effects. *J. Chem. Theory Comput.* **2005**, *1*, 581–589.

(17) Hohenberg, P.; Kohn, W. Inhomogeneous Electron Gas. *Phys. Rev.* **1964**, *136*, B864–B871.

(18) Kohn, W.; Sham, L. J. Self-Consistent Equations Including Exchange and Correlation Effects. *Phys. Rev.* **1965**, *140*, A1133–A1138.

(19) Perdew, J. P.; Wang, Y. Accurate and simple density functional for the electronic exchange energy: Generalized gradient approximation. *Phys. Rev. B* **1986**, *33*, 8800–8802.

(20) Becke, A. D. Density-functional thermochemistry. III. The role of exact exchange. *J. Chem. Phys.* **1993**, *98*, 5648–5652.

(21) Lee, C.; Yang, W.; Parr, R. G. Development of the Colle-Salvetti correlation-energy formula into a functional of the electron density. *Phys. Rev. B* **1988**, *37*, 785–789.

(22) Vosko, S. H.; Wilk, L.; Nusair, M. Accurate spin-dependent electron liquid correlation energies for local spin density calculations: a critical analysis. *Can. J. Phys.* **1980**, *58*, 1200–1211.

(23) Schäfer, A.; Huber, C.; Ahlrichs, R. Fully optimized contracted Gaussian basis sets of triple-ζ valence quality for atoms Li to Kr. *J. Chem. Phys.* **1994**, *100*, 5829–5835.

(24) Hartree, D. R. The wave mechanics of an atom with a non-coulomb central field. I. Theory and methods. *Proc. Cambridge Phil. Soc.* **1928**, *25*, 89–110.

(25) Fock, V. Näherungsmethode zur Lösung des quantenmechanischen Mehrkörperproblems. *Z. Phys.* **1930**, *61*, 126–148.

(26) Jensen, F. Polarization consistent basis sets: Principles. *J. Chem. Phys.* **2001**, *115*, 9113–9125.

(27) Jensen, F. Polarization consistent basis sets. II. Estimating the Kohn-Sham basis set limit. *J. Chem. Phys.* **2002**, *116*, 7372–7379.

(28) Jensen, F. Polarization consistent basis sets. III. The importance of diffuse functions. *J. Chem. Phys.* **2002**, *117*, 9234–9240.

(29) Jensen, F. Estimating the Hartree-Fock limit from finite basis set calculations. *Theor. Chem. Acc.* **2005**, *113*, 267–273.

(30) Møller, C.; Plesset, M. S. Note on an Approximation Treatment for Many-Electron Systems. *Phys. Rev.* **1934**, *46*, 618–622.

(31) Weigend, F.; Häser, M. RI-MP2: first derivatives and global consistency. *Theor. Chem. Acc.* **1997**, *97*, 331–340.

(32) Weigend, F.; Häser, M.; Patzelt, H.; Ahlrichs, R. RI-MP2: optimized auxiliary basis sets and demonstration of efficiency. *Chem. Phys. Lett.* **1998**, *294*, 143–152.

(33) Grimme, S. Improved second-order Møller-Plesset perturbation theory by separate scaling of parallel- and antiparallel-spin pair correlation energies. *J. Chem. Phys.* **2003**, *118*, 9095–9102.

(34) Purvis, G. D., III; Bartlett, R. J. A full coupled-cluster singles and doubles model: The inclusion of disconnected triples. *J. Chem. Phys.* **1982**, *76*, 1910–1918.

(35) Raghavachari, K.; Trucks, G. W.; Pople, J. A.; Head-Gordon, M. A fifth-order perturbation comparison of electron correlation theories. *Chem. Phys. Lett.* **1989**, *157*, 479–483.

(36) Dunning, T. H., Jr. Gaussian basis sets for use in correlated molecular calculations. I. The atoms boron through neon and hydrogen. *J. Chem. Phys.* **1989**, *90*, 1007–1023.

(37) Kendall, R. A.; Dunning, T. H., Jr; Harrison, R. J. Electron affinities of the first-row atoms revisited. Systematic basis sets and wave functions. *J. Chem. Phys.* **1992**, *96*, 6796–6806.

(38) Peterson, K. A.; Dunning, T. H., Jr. Accurate correlation consistent basis sets for molecular core-valence correlation effects: The second row atoms Al-Ar, and the first row atoms B-Ne revisited. *J. Chem. Phys.* **2002**, *117*, 10548–10560.

(39) Halkier, A.; Helgaker, T.; Jørgensen, P.; Klopper, W.; Koch, H.; Olsen, J.; Wilson, A. K. Basis-set convergence in correlated calculations on Ne, N_2, and H_2O. *Chem. Phys. Lett.* **1998**, *286*, 243–252.

(40) Goodson, D. Z. Extrapolating the coupled-cluster sequence toward the full configuration-interaction limit. *J. Chem. Phys.* **2002**, *116*, 6948–6956.

(41) Deglmann, P.; Furche, F.; Ahlrichs, R. An efficient implementation of second analytical derivatives for density functional methods. *Chem. Phys. Lett.* **2002**, *362*, 511–518.

(42) Iliaš, M.; Saue, T. An infinite-order two-component relativistic Hamiltonian by a simple one-step transformation. *J. Chem. Phys.* **2007**, *126*, 064102.

(43) Werner, H.-J. et al. MOLPRO, version 2006 1, a package of ab initio programs, 2006. See http://www.molpro.net (accessed June 19, 2008).

(44) Hampel, C.; Peterson, K. A.; Werner, H.-J. A comparison of the efficiency and accuracy of the quadratic configuration interaction (QCISD), coupled cluster (CCSD), and Brueckner coupled cluster (BCCD) methods. *Chem. Phys. Lett.* **1992**, *190*, 1–12.

(45) Deegan, M. J. O.; Knowles, P. J. Perturbative corrections to account for triple excitations in closed and open shell coupled cluster theories. *Chem. Phys. Lett.* **1994**, *227*, 321–326.

(46) Ahlrichs, R.; Bär, M.; Häser, M.; Horn, H.; Kölmel, C. Electronic structure calculations on workstation computers: The program system Turbomole. *Chem. Phys. Lett.* **1989**, *162*, 165–169.

(47) Häser, M.; Ahlrichs, R. Improvements on the direct SCF method. *J. Comput. Chem.* **1989**, *10*, 104–111.

(48) Treutler, O.; Ahlrichs, R. Efficient molecular numerical integration schemes. *J. Chem. Phys.* **1995**, *102*, 346–354.

(49) von Arnim, M.; Ahlrichs, R. Geometry optimization in generalized natural internal coordinates. *J. Chem. Phys.* **1999**, *111*, 9183–9190.

(50) Hättig, C.; Weigend, F. CC2 excitation energy calculations on large molecules using the resolution of the identity approximation. *J. Chem. Phys.* **2000**, *113*, 5154–5161.

(51) Hättig, C.; Hellweg, A.; Köhn, A. Distributed memory parallel implementation of energies and gradients for second-order Møller-Plesset perturbation theory with the resolution-of-the-identity approximation. *Phys. Chem. Chem. Phys.* **2006**, *8*, 1159–1169.

(52) Jensen, H. J. A. et al. Dirac, a relativistic ab initio electronic structure program, Release DIRAC08.beta, 2008. See http://dirac.chem.sdu.dk (accessed June 19, 2008).

(53) Eichkorn, K.; Weigend, F.; Treutler, O.; Ahlrichs, R. Auxiliary basis sets for main row atoms and transition metals and their use to approximate Coulomb potentials. *Theor. Chem. Acc.* **1997**, *97*, 119–124.

(54) Feller, D. The role of databases in support of computational chemistry calculations. *J. Comput. Chem.* **1996**, *17*, 1571–1586.

(55) Schuchardt, K. L.; Didier, B. T.; Elsethagen, T.; Sun, L.; Gurumoorthi, V.; Chase, J.; Li, J.; Windus, T. L. Basis Set Exchange: A Community Database for Computational Sciences. *J. Chem. Inf. Model.* **2007**, *47*, 1045–1052.

(56) Shahbazian, S.; Zahedi, M. Towards a complete basis set limit of Hartree-Fock method: correlation-consistent versus polarized-consistent basis sets. *Theor. Chem. Acc.* **2005**, *113*, 152–160.

(57) Boese, A. D.; Martin, J. M. L.; Handy, N. C. The role of the basis set: Assessing density functional theory. *J. Chem. Phys.* **2003**, *119*, 3005–3014.

(58) Schäfer, A.; Horn, H.; Ahlrichs, R. Fully optimized contracted Gaussian basis sets for atoms Li to Kr. *J. Chem. Phys.* **1992**, *97*, 2571–2577.

(59) Weigend, F.; Furche, F.; Ahlrichs, R. Gaussian basis sets of quadruple zeta valence quality for atoms H-Kr. *J. Chem. Phys.* **2003**, *119*, 12753–12762.

(60) Klopper, W.; Noga, J.; Koch, H.; Helgaker, T. Multiple basis sets in calculations of triples corrections in coupled-cluster theory. *Theor. Chem. Acc.* **1997**, *97*, 164–176.

(61) Karton, A.; Taylor, P. R.; Martin, J. M. L. Basis set convergence of post-CCSD contributions to molecular atomization energies. *J. Chem. Phys.* **2007**, *127*, 064104.

(62) Lee, T. J.; Taylor, P. R. A diagnostic for determining the quality of single-reference electron correlation methods. *Int. J. Quantum. Chem., Quantum. Chem. Symp.* **1989**, *23*, 199–207.

(63) Janssen, C. L.; Nielsen, I. M. B. New diagnostics for coupled-cluster and Møller-Plesset perturbation theory. *Chem. Phys. Lett.* **1998**, *290*, 423–430.

(64) Lévy-Leblond, J.-M. Nonrelativistic particles and wave equations. *Commun. Math. Phys.* **1967**, *6*, 286–311.

(65) Reiling, S.; Brickmann, J.; Schlenkrich, M.; Bopp, P. A. 1,2-Ethanediol: The Problem of Intramolecular Hydrogen Bonds. *J. Comput. Chem.* **1996**, *17*, 133–147.

(66) Jensen, F. The magnitude of intramolecular basis set superposition error. *Chem. Phys. Lett.* **1996**, *261*, 633–636.

(67) Senent, M. L.; Wilson, S. Intramolecular Basis Set Superposition Errors. *Int. J. Quantum Chem.* **2001**, *82*, 282–292.

(68) Boys, S. F.; Bernardi, F. The calculation of small molecular interactions by the differences of separate total energies. Some procedures with reduced errors. *Mol. Phys.* **1970**, *19*, 553–566.

(69) Dos Santos, H. F.; Rocha, W. R.; De Almeida, W. B. On the evaluation of thermal corrections to gas phase ab initio relative energies: implications to the conformational analysis study of cyclooctane. *Chem. Phys.* **2002**, *280*, 31–42.

CT800182E